

# Modeling Jupiter's Internal Electrostatic Discharge Environment

Robin W. Evans\*

Gibbel Corporation, Montrose, California 91020

and

Henry B. Garrett†

Jet Propulsion Laboratory, California Institute of Technology, Pasadena, California 91109

**A method is provided for determining the internal electrostatic discharge environment of Jupiter for future Jovian missions. Jupiter's severe radiation environment is believed to have caused at least 42 internal electrostatic discharge events during the Voyager 1 flyby. A set of simple tools is presented that allows estimates of the peak electron fluxes and mission fluences for both circular orbits and for equatorial flyby missions with a factor of 2–3 variation. These tools are based on the Divine–Garrett model (Divine, T. N., and Garrett, H. B., "Charged Particle Distributions in Jupiter's Magnetosphere," *Journal of Geophysical Research*, Vol. 88, No. A9, 1983, pp. 6889–6903) and recent data from the Galileo mission. Sample applications are presented.**

## Nomenclature

$B$	=	magnetic field strength, G
$E$	=	electric field strength, V/m, or energy, eV
$L$	=	magnetic shell parameter, RJ
$l$	=	system 3 longitude, deg
$M$	=	magnetic dipole moment, A m <sup>2</sup>
$R_J$	=	Jovian equatorial radius
$\alpha$	=	pitch angle, deg
$\varepsilon$	=	dielectric constant
$\sigma$	=	conductivity, ( $\Omega \cdot \text{m}$ ) <sup>-1</sup>
$\sigma_o$	=	dark conductivity, ( $\Omega \cdot \text{m}$ ) <sup>-1</sup>
$\sigma_r$	=	radiation-induced conductivity, ( $\Omega \cdot \text{m}$ ) <sup>-1</sup>
$\tau$	=	characteristic time constant, s
$\omega$	=	angular frequency, deg/day

## Introduction

**A**LTHOUGH anomalies caused by internal electrostatic discharge (IESD) are currently an important concern for Earth-based missions, IESD is not often considered a hazard for interplanetary missions. During the Voyager 1 flyby of Jupiter, a number of anomalies were observed that were ultimately attributed to IESD. IESD is a concern for any mission that must pass through a region of intense, high-energy electrons such as found at the Earth and Jupiter. This paper will revisit the effects observed on Voyager and review what we now know of the Jovian IESD environment based on Galileo observations. A specific example of a mission that could benefit from these findings is Europa Orbiter, a mission to orbit the Jovian moon Europa. Following a brief discussion of the major issues associated with IESD, the Jovian environment, and the original Voyager 1 observations, this paper will present several tools for evaluating IESD for both Jovian orbiters and flyby missions. In addition, recent observations from Galileo in the vicinity of Europa will be discussed that shed light on the temporal variability of the Jovian IESD environment. Together, these results should provide a more complete understanding of the IESD threat around one of the most important bodies in the solar system, Jupiter, and hopefully lead to more reliable spacecraft.

Received 21 December 2001; revision received 6 May 2002; accepted for publication 4 June 2002. Copyright © 2002 by the American Institute of Aeronautics and Astronautics, Inc. The U.S. Government has a royalty-free license to exercise all rights under the copyright claimed herein for Governmental purposes. All other rights are reserved by the copyright owner. Copies of this paper may be made for personal or internal use, on condition that the copier pay the \$10.00 per-copy fee to the Copyright Clearance Center, Inc., 222 Rosewood Drive, Danvers, MA 01923; include the code 0022-4650/02 \$10.00 in correspondence with the CCC.

\*Scientist, 2550 Honolulu Boulevard, Suite 102; rwe@bb5.jpl.nasa.gov.  
†Principal, Reliability Engineering Office, M/S 122-107, 4800 Oak Grove Drive; Henry.Garrett@jpl.nasa.gov. Associate Fellow AIAA.

## IESD

First consider the definition of IESD. Internal charging as used here refers to the accumulation of electrical charge on interior, ungrounded metals, or in dielectrics inside a spacecraft. The key difference between "internal" and "external/surface" charging is that surface electrostatic discharges often are loosely coupled to victim circuits, whereas internal discharges may occur directly adjacent to victim circuits. Figure 1 shows electron and proton ranges in aluminum vs energy. Because most satellites have an outer shell with aluminum equivalent thickness of 30 or more mils, internally deposited electrons usually have to have an external energy greater than 500 keV. Thus, electrons with 500 keV of energy or more are considered to be the primary environment responsible for internal charging problems. Although the fluxes are normally lower at these higher energies, any internal electrostatic discharge they might cause is closer to victim electronics than external electrostatic discharges (ESD) and, therefore, can cause significant upset or damage to satellite electronics. Internal charging can, however, occur under thinner protective layers (as thin as a thermal blanket) so that the energy threshold for internal charging can be as low as 100 keV.

Except for bulk conducting materials, charge will be deposited over a finite depth because any particle with energy profile over a few electron volts will penetrate the surface. The depth of penetration and charge deposition is a function of stopping power, energy of the impinging particles, and any electric fields normal to the surface. A common spacecraft surface configuration that will exhibit this behavior consists of an exposed dielectric material with a conductive backing connected to the spacecraft ground.<sup>1</sup> Charge will accumulate (or diffuse away) in the dielectric over time as a function of the conductivity of the material and the imposed electric fields. If the charge accumulating in the dielectric induces a field greater than the breakdown strength of the material (typically of the order of  $10^5$ – $10^6$  V/cm), a discharge can occur within the material or from the interior of the dielectric to one of its surfaces.

Of equal importance in determining the likelihood of an IESD as the electron fluence is the time it takes for the electric field to come to a constant value. That time period is characterized by the constant  $\tau = \varepsilon/\sigma$ , where  $\sigma = \sigma_o + \sigma_r$ . For many materials,  $\tau$  ranges from 10 to  $10^3$  s. Some common dielectric materials used in satellites have time constants of  $3 \times 10^5$  s or more. In regions where the dose rate is high (enhancing the radiation conductivity), the  $E$  field comes to equilibrium rapidly. In lightly irradiated regions, where the time constant is long (the dark conductivity dominates), the field takes a long time to reach equilibrium. Depending on the dielectric constant and resistivity, as a rule of thumb,  $10^{10}$ – $10^{11}$  electrons/cm<sup>2</sup> on the interior of a spacecraft may cause internal discharges (for example, Ref. 2). Electron energies of importance are between 100 keV and 3 MeV for typical spacecraft construction and most Earth orbits. Charging times at these energies and at the flux levels common

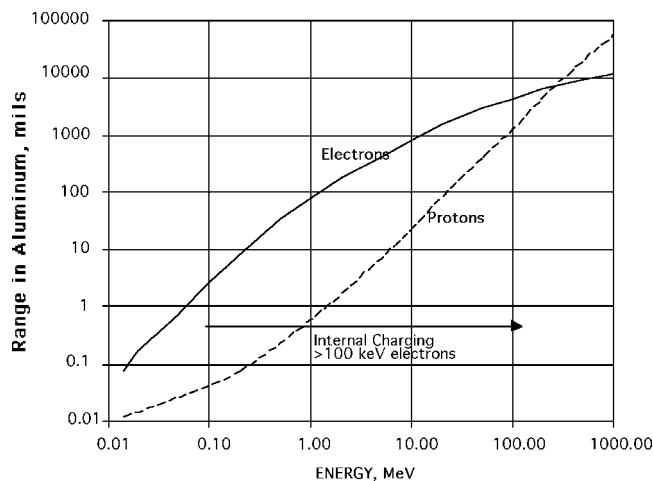


Fig. 1 Approximate average electron and proton penetration ranges in aluminum.<sup>19</sup>

to geosynchronous orbit would be from about 3 to 10 h. (Jovian levels are discussed hereafter.) At lower charging rates, material conductivity often leaks off the charge so that internal charging would not be a problem.

### Divine-Garrett Jovian Radiation Model

The next issue to be considered is the Jovian radiation environment. Jupiter has the strongest magnetic field in the solar system. Because the ability to trap particles magnetically is a function of the magnetic strength, it is little wonder then that it has the most intense radiation belts yet observed. To date, the principle engineering model of these radiation belts is the Divine-Garrett formulation.<sup>3</sup> This model can be used to estimate the expected IESD electron fluence levels at Jupiter. (Note that, as will be discussed, the model is currently undergoing revision to reflect the recent Galileo observations at Jupiter.)

Jupiter's magnetosphere has been known since about 1960, when, in analogy with early spacecraft observations of the Earth's radiation belts, it was realized that the Jovian uhf radio emissions could be interpreted in terms of trapped energetic electrons.<sup>4</sup> The successful encounters of the Pioneer 10 and 11 spacecraft with the Jovian magnetosphere gave rise to a number of quantitative models describing various aspects of the Jovian magnetosphere.<sup>5,6</sup> In particular, magnetic field models by Smith et al.<sup>7</sup> and Acuna and Ness<sup>8,9</sup> began to delineate the substantial differences that exist between the Jovian and terrestrial magnetospheres. Pronounced wavelike variations in the high-energy particle fluxes led to the proposal that the Jovian magnetosphere was distorted into a thin disk and that this thin disk was populated by a cold plasma consisting of heavy ions originating from Io. The passage of the Voyager 1 and 2 spacecraft further refined the particle and field observations. Subsequently, theoretical models have helped to interpret the observations and have led to the development of Jovian magnetospheric models capable of being used to make practical predictions about the environment around Jupiter. (See reviews in Refs. 5 and 6.)

Based on remote radio emission data and in-situ particle data from the Pioneers and Voyagers, Divine and Garrett<sup>3</sup> formulated a comprehensive engineering model of the Jovian radiation environment suitable for IESD calculations. The basic variables in the model (e.g., magnetic  $L$  shell, local field strength  $B$ , and pitch angle  $\alpha$  with respect to the field line) are determined by Jupiter's magnetic field. A 15-coefficient, spherical harmonic magnetic field model, the O4 model, derived from the fluxgate magnetometer on Pioneer 11 (Refs. 8 and 9) was used for this purpose to generate the radiation model components. For typical calculations, however, a simple dipole model is quite adequate. (The O4 model does not include the magnetodisk.) The dipole moment of that model was assumed to have the value  $M = 1.535 \times 10^{27}$  A m<sup>2</sup> = 4.218 G-R<sup>3</sup>. The value of the Jovian equatorial radius was assumed to be  $1 R_J = 7.1492 \times 10^7$  m. The common angular speed of rotation of Jupiter's internal magnetic field and of a meridian of constant longitude  $l$  in system 3 (1965) coordinates was assumed to be

$\omega = 870.5366$  deg/day  $\approx 12.6$  km/s- $R_J$ . In this system,  $l$ , the longitude, increases westward. Conversions to other coordinate systems may be derived from Seidelmann and Divine.<sup>10</sup>

The principal radiation belt populations included in the model are electrons ( $E > 0.06$  MeV) and protons ( $E > 0.6$  MeV). The range of applicability of the energetic electron model, the component of interest to this study, extends to the Jovian magnetopause, whereas that of the protons extends out to  $L = 12$ . The electron model includes a pitch angle dependency within  $L = 16$ , but is considered isotropic beyond that point. For the inner electron and proton models, the independent variables, magnetic  $L$  shell, local field strength  $B$ , pitch angle  $\alpha$  with respect to the field line, and particle kinetic energy  $E$  were utilized. The model populations are assumed independent of time, longitude, and direction azimuth about the field line, as appropriate for stably trapped populations. The reader is referred to Ref. 3 for a complete description of the components of the model.

### Voyager 1 Power-On Resets

During the Voyager 1 flyby of Jupiter on 5 September 1977 (Refs. 11 and 12) numerous anomalies were observed, most of which were determined to be related to 42 power-on resets within the flight data subsystem (FDS). These power on resets (POR) were subsequently attributed to internal charging. In particular, it was postulated that  $\sim$ MeV electrons had penetrated the surface of a cable and built up a charge sufficient to cause arcing. Analysis of Spacecraft Charging at High Altitudes Satellite (SCATHA), Combined Release and Radiation Effects Satellite (CRRES), and Defense Surveillance Program Satellites (DSP) data<sup>13</sup> showed similar effects. Laboratory studies by Leung,<sup>14</sup> Frederickson et al.,<sup>2</sup> Fredrickson,<sup>15,16</sup> and others demonstrated that internal charging was a potential source of discharges. As a result, a series of IESD experiments were flown on the CRRES spacecraft in 1990-1991 (Ref. 2). These experiments, which exposed a variety of configurations of isolated conducting surfaces and dielectrics to the Earth's radiation environment, demonstrated the reality of this effect. Typically, IESD occurred for fluences above  $10^{10}$  electrons/cm<sup>2</sup> in a 10-h orbit.

Upsets in the Voyager POR system are believed to be due to IESD. The Voyager FDS was an onboard computer containing a volatile memory system. Pre-launch, there was concern that powerline undervoltage transients could cause malfunctions of the memory and computer operations with no warning of the malfunctions. To avoid the problem, a POR system was incorporated into the spacecraft's FDS. The key element was an undervoltage sensor that continually monitored the power supply voltage. If an undervoltage occurred, the sensor sent a digital signal to the delay logic electronics, which stopped any processing, stopped the internal clock, reinitialized the computations as needed, waited a period of time, and then restarted computer activity if the undervoltage condition had ceased. The minimum period of time lost was about 175 ms. These 175-ms outages were identified by gaps in the data stream and by 175-ms discrepancies in the timing of spacecraft activities.

Figure 2 illustrates the spatial distribution of the PORs. The timing of the PORs suggested an environmental origin because they occurred with greater frequency as the spacecraft went deeper into the Jupiter plasma environment and decreased as the spacecraft departed, the cause of the anomalies perhaps being electrostatic discharges. To validate this hypothesis, a ground test of the POR circuit was performed to determine its sensitivity to electrical transients. It was found that the sensitive element was an input buffer in the processor delay logic circuitry located in an electronic circuit board about 20 cm away from the undervoltage sensor circuitry. Because the interconnecting wiring was routed in common with other system wiring, it was postulated that ESD noise currents were carried by another wire into the spacecraft and passed near the POR interconnecting wiring. To test this, a 200-mA pulse with a risetime of 20 ns was injected into the adjacent 60-cm wire. This caused a 17-V, 20-ns pulse on the processor delay logic and triggered the circuit. An 8-A, 2- $\mu$ s current pulse caused a 3-V, 5- $\mu$ s voltage pulse on the processor delay logic warning and triggered the circuit. The current pulse slopes were 10- and 4-A/ $\mu$ s, respectively, that is, the rates were roughly comparable. Although not conclusive, these results support

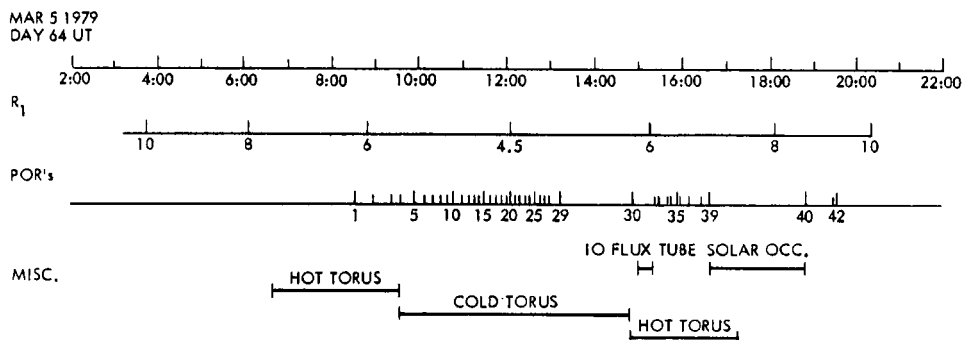


Fig. 2 Temporal and spatial occurrences of the 42 Voyager 1 POR anomalies during the 5 March 1979 flyby.<sup>11</sup>

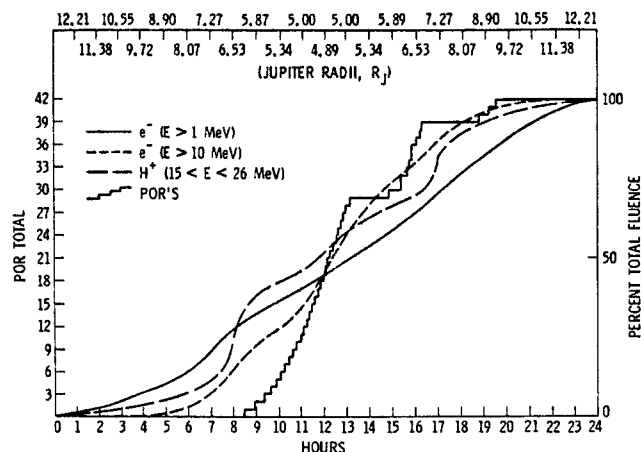


Fig. 3 Comparisons of the cumulative occurrence frequency of the 42 Voyager 1 POR anomalies vs the cumulative high-energy electron ( $E > 1$  MeV and  $E > 10$  MeV) and proton ( $15 \text{ MeV} < E < 26 \text{ MeV}$ ) fluences.<sup>11</sup>

discharge as a likely cause of the POR upsets because pulses of this kind are seen from irradiated insulators in ground-based tests.

Estimates of surface charging in the Jovian environment<sup>11,17</sup> indicated that surface charging was not the likely cause of the Voyager PORs. The predicted surface potentials did not follow the observed asymmetric anomaly pattern. In particular, the anomalies started at about  $5.8 R_J$  on the inbound leg to perijove but continued occurring on the outbound leg to  $9 R_J$ , well beyond the expected surface charging region. Rather it was proposed that the pattern might follow the time-integrated high-energy electron fluence. To test this assumption, the total fluence of electrons at  $E > 1$  MeV and  $E > 10$  MeV and protons  $15 \text{ MeV} < E < 26 \text{ MeV}$  were computed as a function of time. The resulting normalized curves are plotted vs the cumulative sum of Voyager POR anomalies in Fig. 3. (Cumulative was used as the charge buildup associated with IESD is a cumulative process.) Indeed, as Fig. 3 implies, IESD is a possible source of the Voyager anomalies in a temporal sense because the 10-MeV energetic electron fluence does roughly follow the pattern of POR events. The major evidence for buried charge as the cause, however, comes from an estimate of the charge deposited in each arc that would be necessary to cause the observed POR upsets. That argument is developed next.

As an estimate of the IESD environment encountered during the Voyager 1 flyby, consider the following:

- 1) For 42 events in approximately 12 h,  $t \approx 10^3 \text{ s/event}$ .
- 2) For  $4.5\text{--}9 R_J$  and 1-MeV electrons,  $J \approx 7 \times 10^7 \text{ e/cm}^2 \cdot \text{s}$ .
- 3) Therefore, the total available charge was  $q(\text{event}) \approx 7 \times 10^{10} \text{ e/cm}^2 \cdot \text{event}$ .

In the ground testing, a POR could be triggered indirectly by a current in a source wire adjacent to the POR circuit wire by a current rising from 0 to 200 mA in 20 ns. The minimal charge to do this is calculated as follows. (A triangular waveform is assumed in step 1.)

- 1)  $\Delta t \approx 20 \text{ ns}$  and  $I \approx 200 \text{ mA}$  leads to  $Q(\text{event}) \approx 0.5 \times 4 \times 10^{-9} \text{ C} = 2 \times 10^{-9} \text{ C}$ .
- 2) As  $e = 1.6 \times 10^{-19} \text{ C}$  leads to  $Q(\text{event}) \approx 1.3 \times 10^{10} \text{ e/event}$ .

Although these values are probably only accurate to an order of magnitude, they imply that there should be sufficient electron fluence for  $E > 1$  MeV onto a  $1\text{-cm}^2$  area behind a typical 2-mm (80-mil) aluminum surface to account for the observed Voyager 1 POR events. As discussed, Frederickson et al.<sup>2</sup> found similar fluence levels in a 10-h period were likely to generate IESD on the CRRES mission.

### Jovian IESD Tools

In previous papers,<sup>3,18,19</sup> simple tools were developed for helping projects determine regions of concern for surface charging at the Earth and Jupiter and IESD at the Earth. This paper adds tools for IESD at Jupiter. Figures 4–6 are contour plots of the 1-, 10-, and 100-MeV electron fluences, respectively, at the indicated latitudes and radial distances in 10 h. As such, Figs. 4–6 also provide rough estimates of the fluxes and fluences to be expected for circular orbits with those radii and inclinations. Given the 11-deg tilt and  $0.1 R_J$  offset of the Jovian magnetic field/radiation belts, the results for a specific circular orbit would be somewhat different and dependent on orbital phasing relative to Jupiter's spin; levels would need to be calculated for the actual orbit. Even so, Figs. 4–6 are useful for estimating when fluence levels might be high enough to cause IESD. For example, a spacecraft with a typical level of shielding of about 2 mm (80 mil) of aluminum (corresponding to  $\sim 1$ -MeV electrons) would likely begin to experience IESD anomalies for equatorial orbits inside approximately  $15\text{--}20 R_J$  according to Fig. 4. At  $\sim 2.2 \text{ cm}$  (corresponding to 10-MeV electrons) of shielding, the IESD problem appears to be minimal outside of  $10 R_J$ . (The fluence would be less than  $10^{10} \text{ electrons/cm}^2$  in 10 h.)

Voyager 1 is representative of a type of mission that could experience IESD. Jupiter's gravity assists flybys. For an example of how to use the tools, Figs. 7 and 8 (based on data from Divine<sup>20</sup>) represent the peak fluxes and total fluences for Jovian equatorial flybys with perijoves between 5 and  $50 R_J$  and electron energies from 0.1 to 100 MeV. The peak flux can be used to estimate the worst IESD rate for a given perijove, whereas the mission fluence can be used to estimate the total upsets. Consider shielding levels of about 2 mm (80 mils) of aluminum. For this shield thickness, the maximum flux within  $\sim 15 R_J$  would be  $\sim 10^7\text{--}10^8 \text{ electrons/cm}^2 \cdot \text{s}$ . At these levels, in a 1-h period near perijove, a spacecraft might see 30–40 IESD events on an isolated interior conductor of  $\sim 1\text{-cm}^2$  area (corresponding to the rate Voyager 1 saw). Likewise, from Fig. 7, the total mission fluence for orbits with perijoves between  $5\text{--}15 R_J$  is  $\sim 10^{12} \text{ electron/cm}^2$ . This estimate implies that a mission with perijoves in this range might see upward of 100 events on the same isolated conductor as it passed by Jupiter. For a conductor behind  $\sim 2.2 \text{ cm}$  of shielding, there would likely be only a few upsets for a  $1\text{-cm}^2$  area because 10-MeV or higher energy incident electrons are required. It would probably take upward of a  $10\text{-cm}^2$  area or more of a single conductor to cause a significant number of IESD for this region.

### Galileo IESD

The apparent IESD effects on Voyager 1 were a major concern for the Galileo mission. As a result, several steps were taken to limit

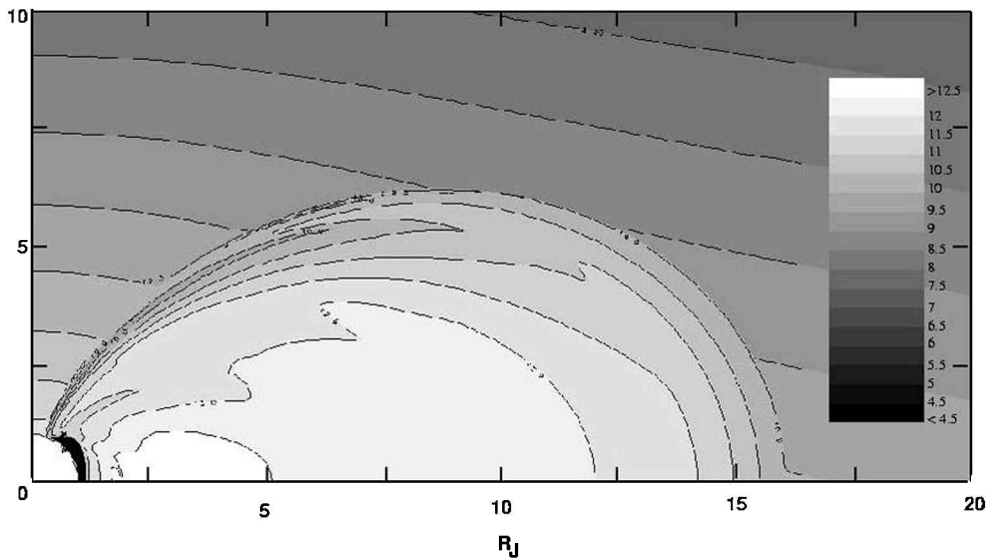


Fig. 4 Contour plot of the  $E > 1$  MeV high-energy electron fluence (log) at Jupiter as estimated from the Divine–Garrett model; fluences (per square centimeter) are for a 10-h period.

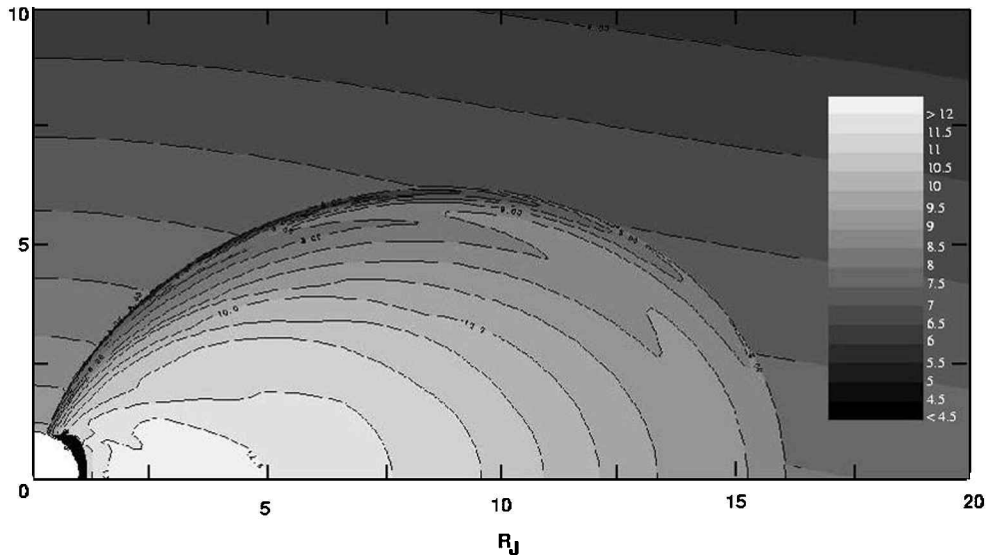


Fig. 5 Contour plot of the  $E > 10$  MeV high-energy electron fluence (log) at Jupiter as estimated from the Divine–Garrett model; fluences (per square centimeter) are for a 10-h period.

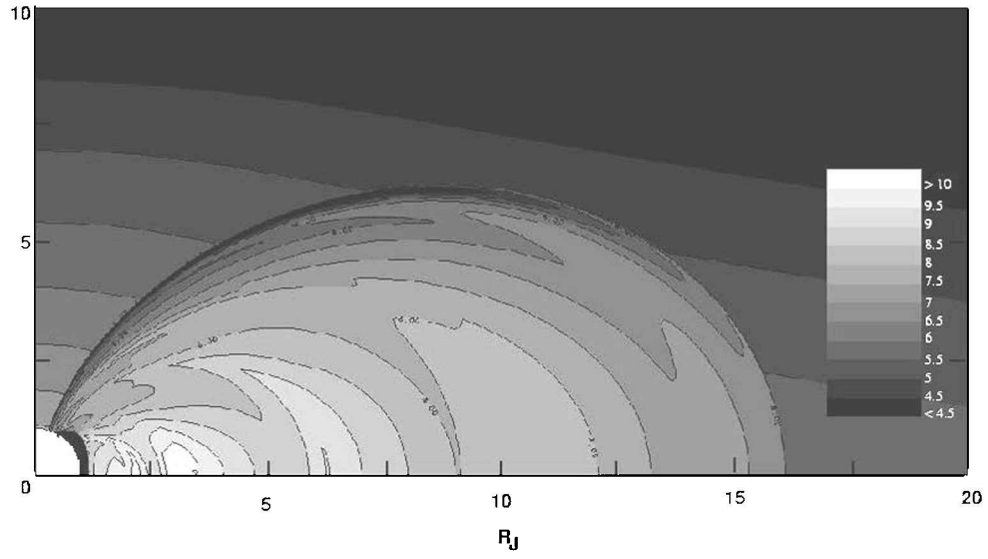


Fig. 6 Contour plot of the  $E > 100$  MeV high-energy electron fluence (log) at Jupiter as estimated from the Divine–Garrett model; fluences (per square centimeter) are for a 10-h period.

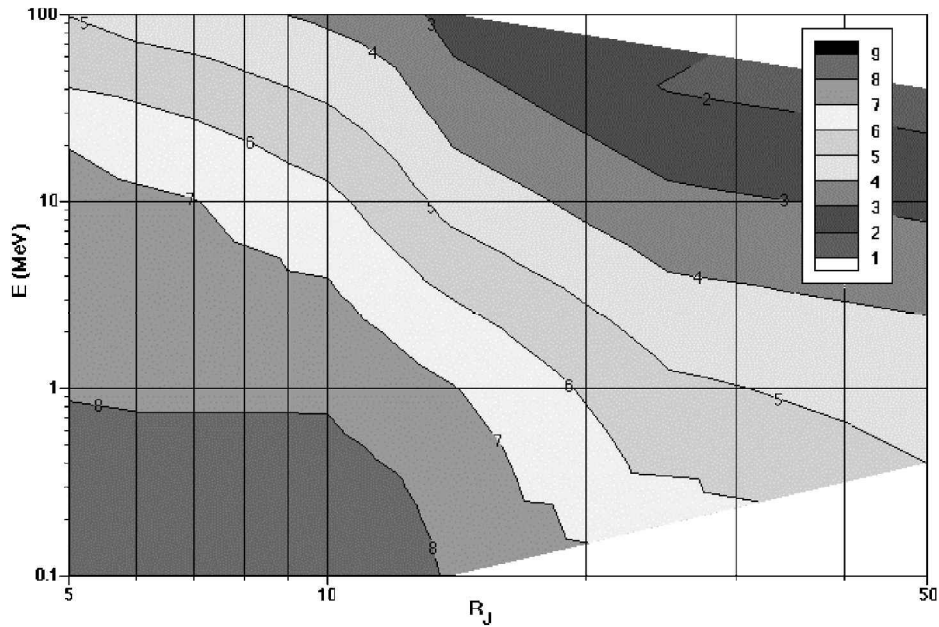


Fig. 7 Contour plot of the peak electron flux (log) as a function of flyby perijove distance and energy. (Note that all flybys are assumed to be in the Jovian equatorial plane<sup>20</sup> and that units are per square centimeter per second.)

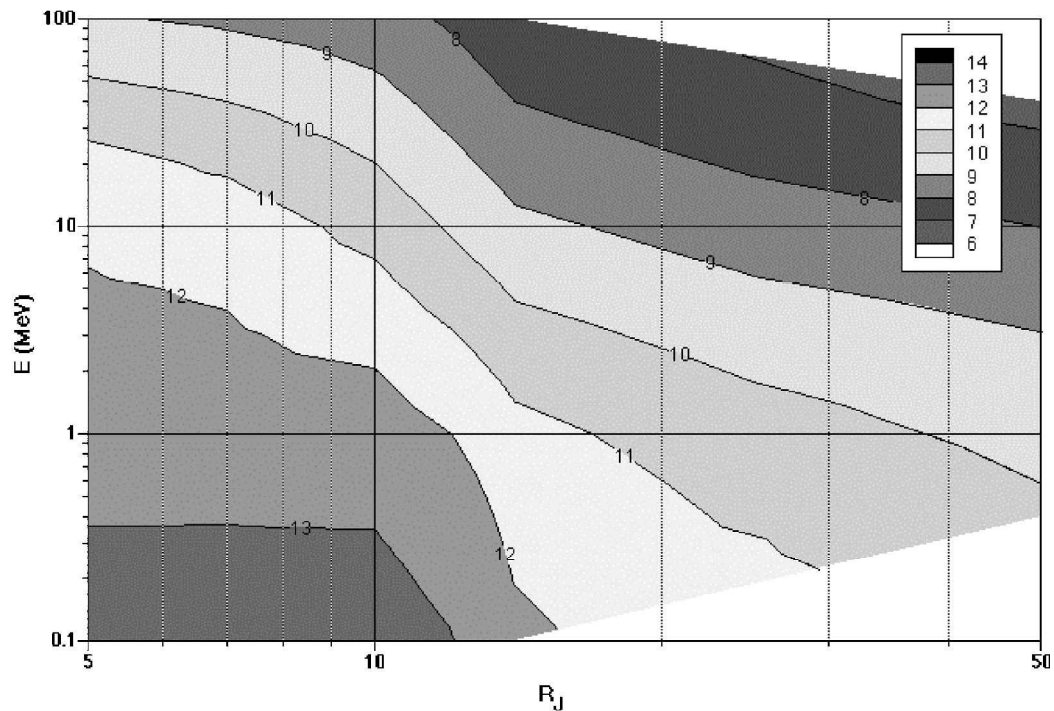


Fig. 8 Contour plot of the total electron fluence (log) as a function of flyby perijove distance and energy. (Note that all flybys are assumed to be in the Jovian equatorial plane<sup>20</sup> and that units are per square centimeter.)

these effects. To evaluate possible effects on Galileo, Leung et al.<sup>21</sup> exposed representative samples of the spacecraft cabling and circuit boards to high-energy electrons. The results demonstrated that IESD could be a real concern for isolated conductors on Galileo. To limit these effects, the approach taken by the project was to require all conductive surfaces to have a resistance of  $<10^{12} \Omega$  relative to spacecraft ground. Isolated conductors were limited to  $<3 \text{ cm}^2$ . Ungrounded conductors with a length greater than 25 cm were also not allowed. Also note that Galileo had an average shielding of  $2.2 \text{ g/cm}^2$  ( $\sim 300$  mils or 0.75 cm of aluminum), corresponding to an electron cutoff of  $\sim 3 \text{ MeV}$ . Because no obvious IESD events have been observed on Galileo, it appears that these steps were successful in eliminating IESD for the Galileo mission.

The Divine-Garrett radiation model<sup>3</sup> provides an average estimate of the IESD environment. Variations in the IESD environment might also be of concern, however. Fortunately, Galileo is currently providing real-time measurements of the Jovian environment. Specific to the IESD environment are high-energy electron measurements by the Johns Hopkins University, Applied Physics Laboratory's Energetic Particle Detector (EPD) at energies of 1.5–10.5,  $E > 2$ , and  $E > 11 \text{ MeV}$  (Ref. 22). In addition, recent work by Fieseler<sup>23</sup> has demonstrated that the Galileo Star Scanner is apparently sensitive to energetic electrons between 5 and 15 MeV. Although the EPD data will ultimately allow spectral measurements of the electron environment, there are numerous temporal gaps. The Star Scanner data, on the other hand, although lacking in energy

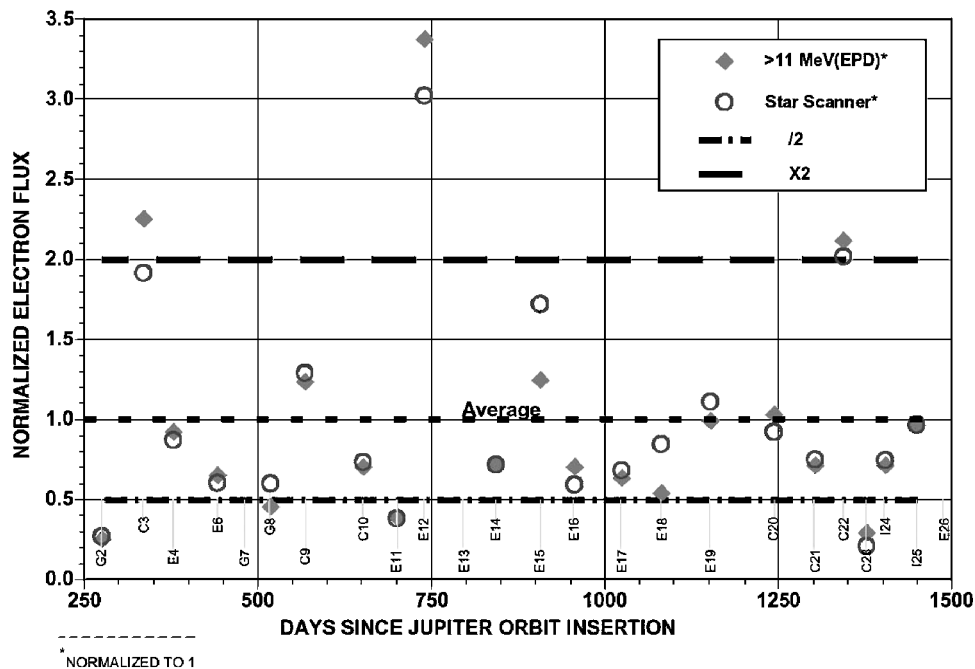


Fig. 9 Normalized energetic electron fluxes (10-min time averages) for  $E > 11$  MeV as measured by the Applied Physics Laboratory's EPD instrument on Galileo up to January 2000; also shown is the normalized Galileo Star Scanner background count rate (10-min time averages) for the same period.

resolution, provide a near-continuous record over the Galileo mission. By the use of the two sets of data time averaged into 10-min intervals, it has been possible to estimate the relative flux variations from orbit to orbit. Figure 9 shows the normalized energetic electron fluxes (10-min time averages) for  $E > 11$  MeV as measured by the Johns Hopkins University, Applied Physics Laboratory's EPD instrument on Galileo.<sup>22</sup> Also shown is the normalized Galileo Star Scanner background count rate (10-min time averages).<sup>23</sup> Of particular significance, Fig. 9 presents the orbit-to-orbit variations for the mission up through January 2000 for the spatial interval 9–10  $R_J$  near Europa's orbit. The key conclusion of Fig. 9 is that the high-energy electron IESD environment appears to vary by a factor of  $\sim 2$ –3 around the average value from orbit to orbit. It is inferred from this that the IESD environment may also vary by a similar factor.

### Conclusions

The objective of this study has been to provide an understanding of the expected IESD environment of Jupiter for future Jovian missions. Jupiter is of interest to the space community because it has a severe radiation environment that is believed to have caused at least 42 IESD events during the Voyager 1 flyby. Based on the Divine-Garrett model of the Jovian radiation environment,<sup>3</sup> a set of simple tools have been presented that allow estimates of the peak electron fluxes and mission fluences for both circular orbits and for equatorial flyby missions. The Divine-Garrett model is an average model. To provide an estimate of the range of values, recent data from the Galileo mission in the vicinity of Europa were used to determine the expected temporal variations in the IESD environment. Based on these results, a factor of 2–3 variation has been estimated. Finally, Galileo apparently has successfully avoided IESD anomalies by implementing a rigorous program that included limiting isolated conductors internal to the spacecraft radiation shield. The methods employed by Galileo to limit IESD were briefly discussed.

### Acknowledgments

The research described in this paper was carried out at the Jet Propulsion Laboratory, California Institute of Technology, under contract with NASA. The authors thank the Johns Hopkins University, Applied Physics Laboratory (W. McEntire and D. Williams) for providing the Energetic Particle Detector data and P. Fieseler of the Galileo Project for providing the Star Scanner data. We also profited greatly from comments by our colleagues A. Whittlesey,

A. R. Frederickson, and W. McAlpine of the Jet Propulsion Laboratory, California Institute of Technology.

### References

- Frederickson, A. R., Cotts, D. B., Wall, J. A., and Bouquet, F. L., *Spacecraft Dielectric Material Properties and Spacecraft Charging*, Vol. 107, Progress in Aeronautics and Astronautics, AIAA, New York, 1986.
- Frederickson, A. R., Holeman, E. G., and Mullen, E. G., "Characteristics of Spontaneous Electrical Discharges of Various Insulators in Space Radiation," *IEEE Transactions in Nuclear Science*, Vol. V-39, No. 6, 1992, pp. 1773–1782.
- Divine, T. N., and Garrett, H. B., "Charged Particle Distributions in Jupiter's Magnetosphere," *Journal of Geophysical Research*, Vol. 88, No. A9, 1983, pp. 6889–6903.
- Drake, F. D., and Havatum, H., "Non-Thermal Microwave Radiation from Jupiter," *Astronomical Journal*, Vol. 64, Oct. 1959, pp. 329, 330.
- Gehrels, T. (ed.), *Jupiter*, Univ. of Arizona Press, Tucson, AZ, 1976.
- Dessler, A. J., (ed.), *Physics of the Jovian Magnetosphere*, Cambridge Planetary Science Series, Cambridge Univ. Press, New York, 1983.
- Smith, E. J., Davis, L., Jr., and Jones, D. E., "Jupiter's Magnetic Field and Magnetosphere," *Jupiter*, edited by T. Gehrels, Univ. of Arizona Press, Tucson, AZ, 1976, pp. 788–829.
- Acuna, M. H., and Ness, N. F., "Results from the GSFC Fluxgate Magnetometer on Pioneer 11," *Jupiter*, edited by T. Gehrels, Univ. of Arizona Press, Tucson, AZ, 1976, pp. 830–847.
- Acuna, M. H., and Ness, N. F., "The Main Magnetic Field of Jupiter," *Journal of Geophysical Research*, Vol. 81, No. 16, 1976, pp. 2917–2922.
- Seidelmann, P. K., and Divine, T. N., "Evaluation of Jupiter Longitudes in System III (1965)," *Geophysical Research Letters*, Vol. 4, No. 4, 1977, pp. 65–68.
- Leung, P., Whittlesey, A. C., Garrett, H. B., Robinson, P. A., Jr., and Divine, T. N., "Environment-Induced Electrostatic Discharges as the Cause of Voyager 1 Power-On Resets," *Journal of Spacecraft and Rockets*, Vol. 23, No. 3, 1986, pp. 323–330.
- Whittlesey, A. C., and Leung, P., "Space Plasma Charging: Lessons from Voyager," AIAA 25th Aerospace Sciences Meeting, Jan. 1987.
- Vampola, A. L., "Thick Dielectric Charging on High-Altitude Spacecraft," *Journal of Electrostatics*, Vol. 20, 1987, pp. 21–30.
- Leung, P., "Discharge Characteristics of a Simulated Solar Array," *IEEE Transactions in Nuclear Science*, Vol. NS-30, 1983, p. 4311.
- Frederickson, A. R., "Radiation Induced Dielectric Charging," *Space Systems and Their Interactions with the Earth's Space Environment*, edited by H. B. Garrett and C. P. Pike, AIAA, New York, 1980, pp. 386–412.
- Frederickson, A. R., "Electrostatic Charging and Discharging in Space Environments," *Proceedings of the 10th International Symposium Discharges and Electrical Insulation in Vacuum*, 1983.

<sup>17</sup>Garrett, H. B., and Hoffman, A., "Comparison of Spacecraft Charging Environments at the Earth, Jupiter, and Saturn," *IEEE Transactions on Plasma Physics*, Special Issue on Space Plasmas, Vol. 28, No. 6, 2000, pp. 2048–2057.

<sup>18</sup>Evans, R., Garrett, H. B., Gabriel, S., and Whittlesey, A. C., "A Preliminary Spacecraft Charging Map for the Near Earth Environment," *Proceedings of the Spacecraft Charging Technology Conference*, edited by R. C. Olsen, Vol. 2, Phillips Lab., U.S. Air Force Material Command, Hanscom AFB, MA, 1989, pp. 615–621.

<sup>19</sup>Whittlesey, A. C., "Avoiding Problems Caused by Spacecraft On-Orbit Internal Charging Effects," NASA HDBK-4002, 1999.

<sup>20</sup>Divine, N., "Flux, Fluence, and Dose for Jupiter Flyby Trajectories," Jet Propulsion Lab., IOM 5217-91-47, California Inst. of Technology, Pasadena, CA, Feb. 1991.

<sup>21</sup>Leung, P. L., Plamp, G. H., and Robinson, P. A., Jr., "Galileo Internal Electrostatic Discharge Program," *Spacecraft Environmental Interactions Technology 1983*, edited by C. K. Purvis, and C. D. Pike, NASA CP-2359/AFGL-TR-85-0018, 1983, pp. 423–435.

<sup>22</sup>Williams, D. J., McEntire, R. W., Jaskulek, S., and Wilken, B., "The Galileo Energetic Particle Detector," *The Galileo Mission*, edited by C. T. Russell, Kluwer Academic, Dordrecht, The Netherlands, 1992, pp. 385–412.

<sup>23</sup>Fieseler, P. D., "The Galileo Star Scanner as an Instrument for Measuring Energetic Electrons in the Jovian Environment," M.S. Thesis, Electrical Engineering Dept., Univ. of Southern California, Los Angeles, Dec. 2000.

D. L. Edwards  
Associate Editor